



# Metallic Nanoparticles and Nano-Based Bioactive Formulations as Nano-Fungicides for Sustainable Disease Management in Cereals

# 16

Hossam S. El-Beltagi, Eslam S. Bendary, Khaled M. A. Ramadan, and Heba I. Mohamed

## Abstract

The main challenge in disease management is to develop and enhance long-term management strategies that diminish the pathogen's ability to pose a threat in the future. The use of fungicides and the planting of resistant varieties are two of the most common ways to combat blast disease. Natural products, botanical extracts, and nanoparticles have been increasingly used as safer antibacterial treatments against plant infections in recent years. Plant tonics and extracts are environmentally safe goods and there is no risk of resistance to their use, as there is with traditional pesticides. The goal of the present chapter was to focus on the effect of the application of these products on the causal agents of cereal diseases. In vitro and in vivo tests were used to assess the impact of plant products or manufactured nanoparticles on crop disease. Application of plant natural compounds

H. S. El-Beltagi (✉)

Agricultural Biotechnology Department, College of Agriculture and Food Sciences, King Faisal University, Al-Ahsa, Saudi Arabia

Biochemistry Department, Faculty of Agriculture, Cairo University, Giza, Egypt

e-mail: [helbeltagi@kfu.edu.sa](mailto:helbeltagi@kfu.edu.sa)

E. S. Bendary

Central Laboratories, King Faisal University, Al-Ahsa, Saudi Arabia

K. M. A. Ramadan

Central Laboratories, King Faisal University, Al-Ahsa, Saudi Arabia

Agricultural Biochemistry Department, Faculty of Agriculture, Ain-Shams University, Cairo, Egypt

H. I. Mohamed

Biological and Geological Sciences Department, Faculty of Education, Ain Shams University, Cairo, Egypt

© The Author(s), under exclusive license to Springer Nature Singapore Pte Ltd. 2022

K. A. Abd-Elsalam, H. I. Mohamed (eds.), *Cereal Diseases: Nanobiotechnological Approaches for Diagnosis and Management*, [https://doi.org/10.1007/978-981-19-3120-8\\_16](https://doi.org/10.1007/978-981-19-3120-8_16)

315

suppressed mycelial growth and conidial growing conditions of fungus considerably *in vitro*, with maximum suppression. Plant tonic application and nanocarbons were likewise the most effective treatments in *in vivo* settings, resulting in a considerable reduction in the area under the disease progress curve (AUDPC) value when compared to the control. The application of plant tonics and natural products resulted in a higher phenolic compound accumulation and higher activity of peroxidase and polyphenol oxidase enzymes than the control. Plant tonic, natural products, and nano-carbon treated rice plants showed no phytotoxicity when compared to the control. The benefits of plant natural products and nanoparticles in suppressing the rice blast disease were confirmed by the findings presented in this chapter. As a result, their application may aid in the development of appropriate management methods and provide the possibility of a cleaner and safer agricultural environment.

---

**Keywords**

Antifungal · Characterization · Fungicide · Fusarium · Plant extract · Nanoparticles · Synthesis

---

## 16.1 Introduction

Nanotechnology is rising in prominence as a result of its numerous agricultural applications (Chowdappa and Gowda 2013; Ul-Haq and Ijaz 2019). Among other disease control measures, nanobiotechnology plays a vital role in early diagnosis, presumed fungicides (nanofungicides), and is effective for fungicide distribution to plants (Mishra and Singh 2015). It is this groundbreaking science that has transformed the green revolution into the green nano-bio revolution. It is centered on two parts: nanomaterial fabrication and implementation (Khan and Rizvi 2014).

Technology enables real-time tracking of agricultural crops for smart farming, resulting in greater production with minimal input (Sharma et al. 2010a, b). Herbicides and fungicides are extensively used, resulting in ecotoxicity and the emergence of novel resistant phytopathogen species (Chen et al. 2015). As a result, there is a pressing need to develop new approaches to managing crop diseases (Vu et al. 2015). The use of environmentally friendly methods that produce less toxic waste is urgently needed on a global scale. Scientists have become more aware of the need to embrace and create “green synthesis” methodologies and techniques as a result of this circumstance. Nanobiotechnology as a green chemistry strategy aims to minimize the manufacturing of hazardous materials using nontoxic and eco-friendly assets. As a result, utilizing biological agents (bio-macromolecules and microorganisms) for nanoparticle production is a unique notion in green chemistry, opening up new paths for studying a wide range of biological species (Chowdappa et al. 2013; Prasad et al. 2018).

Plant extract-based bio-reduction processes for nanomaterial generation involve a variety of biomolecules, including polysaccharides, plant resins, organic

compounds, tannins, pigments, proteins, and enzymes (Nam et al. 2008; Prasad 2014) of green chemistry that connects microbial biotechnology and nanotechnology. Inorganic chemicals are accumulated by microbes either inside or outside the cell, and bio-reduce metals including copper, gold, platinum, silica, and silver to produce nanoparticles (Prasad 2016).

By improving sustainable agriculture, nanoparticles play a critical role in producing better food (Gruère 2012). A wide spectrum of phytopathogens causes damage to crop plants, ornamental plants, and trees, resulting in significant economic damage. Many of them have harmful consequences for human health. In the next half-century, global food demand is predicted to double, posing a significant challenge to food production losses (Tournas 2005).

Because of exhaustion during the application, photodegradation, and off-target deposition, only a trace amount of fungicides and pesticides (0.1%) find the exact site of action; these losses have an impact on the ecosystem and raise production costs. When a fungicide or pesticide is implemented to target pathogens, it may alter their population into new species or strains through genome recombination, resulting in the evolution of new species with resistance to that fungicide or pesticide (Castro et al. 2013; Chowdappa et al. 2013). The best method to deal with this problem right now is to use nanomaterials in illness control, disease monitoring, and precise or controlled dispersion of bioactive agents (Johnston 2010). These nanoparticles are aimed at fixing specific agricultural issues, such as plant protection (disease control) and crop improvement (Ghormade et al. 2011). Nanoparticles' high surface-to-volume proportion makes them more responsive and biochemically active. They attach to pathogen cell walls, causing cell membrane distortion due to high-energy transfer and causing the pathogen to die (Dubchak et al. 2010). These nanoparticles or nanoparticle-based formulations form a robust nanoscale framework that allows agrochemicals to be entrapped and encapsulated for gradual and targeted delivery of their active components while also reducing agrochemical runoff into the environment (Chen and Yada 2011). As a result, this emerging science could play a critical role in global sustainable agriculture. This chapter discusses the importance, production, and properties of nanoparticles (particularly metallic nanoparticles) as well as their use as nanofungicides for long-term disease management in plants (Gruère 2012).

---

## 16.2 Cu Nanoparticles (Cu-NPs) Fungicides Against Fusarium

### 16.2.1 Synthesis and Characterization of Copper Nanoparticles

Copper nanoparticles were created through the use of the cetyltrimethyl ammonium bromide method (Kanhed et al. 2014). The process was optimized for the optimal concentration of copper nitrate and cetyltrimethyl ammonium bromide (CTAB) in terms of nanoparticle stability. The optimization study used 20 mL of copper nitrate at room temperature, with concentration ranges of 0.010–0.100 M for cetyltrimethyl ammonium bromide and 0.0010–0.0100 M for copper nitrate (Bramhanwade et al.

2016). Different concentrations of CTAB solution (0.001–0.01 M) and 20 mL of CTAB solution (0.001–0.01 M) were prepared in isopropyl alcohol. Drop by drop, copper nitrate solution was poured into the CTAB solution while vigorously stirring. Copper nanoparticles have a well-known feature of easily oxidizing in the presence of oxygen. This can be avoided by applying a capping agent to cover the nanoparticles. In this method, the concentrations of copper nitrate and CTAB were adjusted to produce copper nanoparticles. Copper nitrate at 0.003 M was discovered to be the lowest concentration that might support copper nanoparticle production, while CTAB at 0.02 M was determined to be the lowest concentration that might support copper nanoparticle synthesis. Moreover, Kanhed et al. (2014) used a comparable concentration of copper nitrate (0.003 M) but a larger concentration of CTAB to synthesize copper nanoparticles (0.090 M). For the manufacture of copper nanoparticles, different amounts of CTAB were used, including 0.087 M, 0.09 M, and 50% (Zhang and Cui 2009). Upon adding copper nitrate to the CTAB solution with continual swirling and magnetic stirring, the color shift for copper nanoparticles was gloomy violet. Bahadory (2008) attributed the color change to surface plasmonic stimulation in metal nanoparticles. The stability of the CTAB procedure of copper nanoparticle manufacturing was one of its shortcomings (Shah et al. 2014).

To determine the stability of copper nanoparticles, the zeta potential was evaluated. It is based on charge behavior phenomena. Nanoparticles are said to be unstable if their zeta potential value is between  $-30$  and  $+30$ . The stability of generated copper nanoparticles was taken into account when measuring the zeta potential of various concentrations of copper nitrate and CTAB.

### 16.2.2 Antifungal Activity of Cu-NPs Toward *Fusarium*

The use of nanoparticles in a variety of disciplines has a principal impact on society and the global economy. In a continuous flow mode, copper metals were successfully absorbed from polluted water using an alginate-immobilized water hyacinth, i.e., *Eichhornia crassipes*, which serves as a potential biosorbent in acidic media (Bramhanwade et al. 2016). *Fusarium culmorum*, *Fusarium oxysporum*, and *Fusarium equiseti* belong to the *Fusarium* species. In barley and wheat, *F. culmorum* causes pre-emergence cotyledon blight, root rot, foot rot, or head blight (Mesterhazy et al. 2005).

Chickpea wilt, *Fusarium* crown, *Fusarium* head blight, yellows, black point disease, corm rot, root rot, vascular wilt, or damping-off are all plant diseases caused by *F. oxysporum* in spinach, sugarcane, lettuce, prickly pear, tomato, garden pea, pansy, potato, cultivated zinnia, cowpea, and Assam rattlebox. *F. equiseti* is a soil-dwelling parasite that can infect a range of crop seeds, roots, tubers, and fruits. It causes disease in a broad range of crop plants (Raabe et al. 1981).

Copper nanoparticles were tested in vitro for antifungal activity versus three different crop fungal pathogens: *Fusarium* sp., *Fusarium oxysporum*, or *Fusarium equise*. Copper nanoparticles, interestingly, had a lot of effect against the crop pathogenic fungi that were studied. Amphotericin B was utilized as a conventional

antifungal drug for antifungal action. Copper nanoparticles had the most action versus *F. culmorum*, *F. equiseti* or *F. oxysporum*. Kanhed et al. (2014) discovered in vitro antifungal activity of chemically generated copper nanoparticles combined with the marketed antifungal drug Bavistin against four different plant pathogenic fungi, including *F. oxysporum*, *C. lunata*, *A. alternata* and *P. destructiva*. Copper nanoparticles have been known to be successful against a wide variety of plant species.

## 16.3 Iron Nanoparticle Biofabrication and Fungicidal Properties

Iron nanoparticles (FeNPs) are used in magnetic storage devices, ferrofluids, magnetic refrigeration systems (Ahmad et al. 2017), medication administration, hyperthermia, bio-separation, and magnetic resonance imaging (e.g., enzyme-linked immunosorbent assay) (Sophie et al. 2008). FeNPs are used in a variety of applications due to their high magnetism, tiny size, microwave absorption capabilities, and low toxicity (Chang et al. 2011). FeNP has been created using a number of chemical processes. Electrospray synthesis, microemulsions, sonochemical reactions, chemical co-precipitation of iron salts, hydrothermal reactions, sol-gel synthesis, and hydrolysis and thermolysis of precursors are some of the popular methods used for FeNP synthesizing (Albornoz and Jacobo 2006). Numerous scientists have created techniques for green synthesis of Fe<sub>3</sub>O<sub>4</sub> nanoparticles in response to the requirement to produce beneficial formulations of bioactive chemicals utilizing nanomaterials that are both environmentally and economically beneficial (Venkateswarlu et al. 2013). Using phytochemicals to generate iron oxide nanoparticles is also a simple, cost-effective, less poisonous, and environmentally friendly method that has previously been used to make other heavy metal nanoparticles. One of the major components in the antibacterial activity mechanism can be active oxygen types created by these metal oxide materials. In this way, nanoparticles of related metal oxides could be good antibacterial agents (Ales et al. 2009).

### 16.3.1 Plant Extracts Are Used to Produce Iron Oxide Nanoparticles

FeNPs were made utilizing processes that have previously been revealed (Xiulan et al. 2013; Valentin et al. 2014). 6H<sub>2</sub>O was handled by 10% plant extract in a 1:2 ratio with around 0.1 M FeCl<sub>2</sub>. The combination was thoroughly agitated at 100 °C till the greenish hue entirely changed to a deep black solution. The solution was seated for 72 h (on Petri plates) inside a 60 °C oven. Eventually, the blackish dry matter was subjected to several characterization procedures.

#### 16.3.1.1 FeNPs Characterization

Surface plasmon resonance (SPR) uptake transition is the most distinguishing feature of nanoparticles. The yellow-colored reaction mixture turned dark brown

after overnight incubation in the dark. It could be due to the produced nanoparticles' SPR excitation (Gopinatha et al. 2012). The reaction medium of iron chloride and neem extract showed a strong peak at 272 nm, confirming the synthesis of FeNPs. Due to N–H stretching and bending vibration of amine group  $\text{NH}_2$  and O–H overlying and stretching mode of soluble neem leaf extract particles, the Fourier transform IR spectroscopy (FTIR) summary of neem extract and FeNPs exhibited continuous spectrum of about  $3000\text{ cm}^{-1}$  focused at  $3325\text{ cm}^{-1}$ . Methyl C–H stretch is indicated by peaks at  $2916$  and  $2850\text{ cm}^{-1}$ , whereas –CHO group of neem extract is indicated by peaks at  $1728\text{ cm}^{-1}$ . The existence of ester linkages is noted by a sharp peak at  $1725\text{ cm}^{-1}$ , whereas the peaks at  $1522$  and  $1453\text{ cm}^{-1}$  in neem extracts can be attributed to bending vibrations of aromatic nitro compounds and carbonate ions, respectively. As reported earlier (Gotic et al. 2009), the band around  $600\text{ cm}^{-1}$  revealed Fe O extending of FeNPs, indicating the synthesis of nanomaterials. According to the general FTIR image, neem extract has the highest FeNP lowering potential, which has been validated by other investigations.

The FeNPs are grouped and embedded in plant components due to the presence of plant detritus. Nanoparticles were discovered to have an average size of 20–80 nm. SAED (selected area electron diffraction) reveals that FeNPs have a less crystalline structure. Along with FeNPs, bio-coatings were apparent, confirming neem extract's capacity to intervene as a protective coating for FeNPs. In FeNPs, the XRD report reveals a thick downward slope with no sharp peaks. In FeNPs, there were no diffraction pattern peaks associated with the prolonged crystalline form. Rather, a wideband appears, which is characteristic of nebulous and ultra-small crystal structures, with poorly defined diffraction patterns. Previous research on plant extract-based FeNP synthesis has found the same things (Mahnaz et al. 2013; Monalisa and Nayak 2013).

---

## 16.4 Green Synthesis of Zinc Oxide Nanoparticles

Research on nanoparticles is being conducted for its potential, especially in biomedical research, converting agriculture and food wastes to fuel and other useful residues via enzyme nano-bioprocessing, and managing phytopathogens in agriculture using various types of nanocides (Joshi et al. 2019; Ahmad et al. 2020; Nandini et al. 2020; Sangeetha et al. 2017), as well as, drug delivery and bioimaging probes, have proved to have a wide variety of functions in molecular diagnostics, detection, and micro-electronics (Sangeetha et al. 2017). ZnONPs have a unique feature towards bacterial cellulase, which was discovered by studying the creation of hydrogen peroxide on the exterior of ZnONPs (Sharma et al. 2010a, b). The antibacterial properties of nanomaterials have been shown to be more effective than zinc oxide (Kumar et al. 2014). This is because smaller particles have a higher surface-to-volume ratio, with strong antibacterial properties (Kumar et al. 2014; Sharathchandra et al. 2016). ZnONPs are also excellent photocatalysts, which are used to sanitize wastewater and degrade or decrease herbicides and pesticides. Hydrothermal synthesis (Thilagavathi and Geetha 2014), electrochemical approach, mechano-chemical

method, laser ablation, sono-chemical, and polyol methods are some of the commercial routes for ZnONPs manufacture (Muneer et al. 2015), sol-gel method, precipitation method, microwave technique, and vapor-phase transport method (Wang et al. 2014), and by aerosol process (Ozcelik and Ergun 2014). These approaches can be used to make nanoparticles using either chemical or plant-derived materials. The chemical production of metal nanoparticles necessitates the use of synchronized conditions and specific external catalysts. In the case of plant-derived nanoparticles, plants secrete catalysts in the form of co-enzymes that are non-toxic and environmentally friendly reactants, and the reaction takes place at room temperature.

### 16.4.1 Biomaterial Preparation

As a bio-reducing agent, *Eucalyptus globulus* leaves have been chosen for preparation. Plant materials have been shade-dried, cleaned in distilled water, sterilized for 30 s with mercuric chloride (0.1%), and washed five times with sterile water, and then shade-dried again. Using a laboratory blender, the leaves were grinded and utilized for additional research. Fifteen gram of leaf powder has been mixed with 200 mL of deionized water in a flask and incubated for 6 h in a shaker at 80 °C and 1500 rpm. The extract was centrifuged at 10,000 rpm for 10 min before being filtered through Whatman No. 1 paper to achieve a completed volume of 100 mL (Ahmad et al. 2020).

### 16.4.2 Phytosynthesis of Zinc Nanoparticles

In a plant extract solution, 1 mM of zinc nitrate hexahydrate ( $\text{Zn}(\text{NO}_3)_2 \cdot 6\text{H}_2\text{O}$ ) was postponed in a 1:2 ratio with continuous stirring and was agitated at 150 °C for 2–3 h after it was completely dissolved, and the supernatant was discarded. The solid was centrifuged two times at 6000 rpm for 10 min each time before being cleaned and dehydrated at 80 °C for 5–6 h. Dry particles have been kept at room temperature till they change color before being used in future studies (Ahmad et al. 2020).

### 16.4.3 Formation of Zinc Nanoparticles

*E. globulus* leaf extracts were used to make zinc oxide. The color change from colorless to pale yellow confirmed the production of ZnONPs. Other metals have been reported to have color changes that indicate preliminary confirmation of the creation of nanoparticles (Joshi et al. 2019). The presence of ZnONPs is confirmed by the color change in the reaction mixture caused by surface plasmon resonance (Shekhawat et al. 2014). Without any additives or reactions, plant-derived nanomaterials respond quickly at room temperature (Ahmad et al. 2020). When compared to other techniques like physical, chemical, biological, or hybrid

approaches, which require additional power and may introduce dangerous materials that lose their consistency, this method is simple and best suited for measuring biological activity.

#### 16.4.4 Characterization of ZnNPs

SEM pictures of ZnONPs produced utilizing *E. globulus* extract demonstrate that agglomerations of molecules were more common when this technique of production was used. The presence of biological material in the sample is confirmed by the clustered form of nanoparticles. The shape and size of created ZnONPs were discovered utilizing TEM. The resulting ZnONPs were often circular, with some extended particle sizes ranging from 52 to 70 nm. *E. globulus* extracts have previously been shown to behave as an active template during synthesis, avoiding the agglomeration of nanoparticles generated (Gnanasangeetha and Sarala 2013).

#### 16.4.5 Antifungal Activity of ZnONPs

ZnONPs are inorganic nanoparticles that have multiple functions, including antibacterial capabilities. The rate of antifungal activity of ZnONPs produced with *E. globulus* extract was higher than that of Zn bulk material. The activity of ZnONPs had been dose-dependent; at 25 ppm, there was reasonable to fine suppression, followed by a considerable rise in pathogen inhibition at higher concentrations of 50 and 100 ppm (Sharma et al. 2010a, b). In comparison to synthetic ZnONPs, green ZnONPs demonstrated a significant improvement in biological activity against a variety of diseases. Eman et al. (2013) discovered that ZnONPs have antifungal action toward *Microsporium canis*, *Candida albicans*, *Aspergillus fumigatus*, and *Trichophyton mentagrophyte* (Eman et al. 2013). The synergetic effect of ZnONPs and *Eucalyptus globulus* extracts in equal proportion on fungal mycelial growth was assessed. In the instance of *B. dothidea* and *A. mali*, the synergetic activity resulted in a total suppression (100%) of the mycelium at 100 ppm.

##### 16.4.5.1 Fungi Treated with Zinc Nanoparticles Under Microscope

Microscopic examination revealed a rupture at the hyphae tip, which is a site for the generation of new conidia, as well as unconnected conidia in two fungi. The discharge of cellular components could be triggered by damage to the fungal hyphae's surface caused by hyphal contraction. Water-treated hyphae, on the other hand, are unaffected by hyphal injury (Shetty et al. 2019).

##### 16.4.5.2 Effects of ZnONPs on Fungal Mycelia as Examined by SEM

The influence of nanoparticles on developing hyphae was studied under the microscope, and it was discovered that ZnONPs visibly harmed *D. seriata* hyphae, but hyphae handled with water appeared to be unaffected. Under treatment with nanoparticles, distortions and injuries of *D. seriata* hyphal cell wall, degeneration



of sexual organs, and serious damaged hyphal wall layers resulted in severely fractured hyphal wall layers retaining few and shrunken hyphae. Surprisingly, these changes in mycelium structures had no effect on the fungus's life cycle. Villamizar-Gallardo et al. (2016) made a similar observation claiming that produced AgNPs cause significant structural damage to *Aspergillus flavus*, but have no effect on the fungus's life cycle creation.

---

## 16.5 Metallic MgO Nanoparticles

As scientific knowledge has advanced, developing unique alternative techniques for managing soilborne fungal infections has become increasingly desirable (Chen et al. 2020). Magnesium oxide nanomaterials (MgONPs) have been acknowledged by the US Food and Drug Administration as safe disinfection agents with no toxic consequences, and they have significant potential in medical therapies and water disinfection (Chalkidou et al. 2011). Furthermore, earlier research has shown that MgONPs can be employed as microbicide in vitro versus gram-positive (*Staphylococcus aureus*, *Bacillus subtilis*) and gram-negative (*E. coli*) bacterial and fungal pathogens. MgONPs' antibacterial activity is influenced by their pH, size, concentration, or shape (Parizi et al. 2014).

These toxic effect processes, unlike agro-chemicals, quite probably result from immediate physiochemical deletion upon contact, which prevents the disintegration of vegetative fungal spores by producing malic acid and amino acids. Numerous findings have argued that the production of ROS and their buildup in cells is an actual mechanism of metal nanomaterials' antibacterial pathogen defense; this is especially true since ROS formation directly limits a cell's ability to reproduce (Chen et al. 2014). Disinfection of microorganisms is assumed to be based on direct contact among biological cells and nanomaterials (Zhao et al. 2018a, b). Superoxide ion production on the exterior of MgONPs, for example, disrupts peptide connections in the bacterial cell membrane. *Ralstonia solanacearum*, a medicinal and foodborne pathogen, has shown antibacterial potential, successfully lowering agricultural bacterial and fungal infections (Sierra-Fernandez et al. 2017). Despite this, little study has been done on the impacts of MgONPs on fungal infections or complex antimycotic processes. MgONPs could be antifungal by acting directly on fungal cells. Most importantly, an ideal agricultural microbicide would be free of phytotoxicity, which is critical for environmentally friendly and sustainable agriculture. Foliar spray of MgONPs as nanoscale fertilizers or optical absorption boosters substantially boosted crop growth, which was very exciting (Cai et al. 2018). It also showed that Chen et al. (2020) looked into how MgONPs antifungal mechanisms worked against phytopathogenic fungi. This was in comparison to macroscale MgO (mMgO) antifungal mechanisms.

### 16.5.1 Synthesis of MgONPs

Under vigorous stirring, 10 mL of *Carica papaya* L. leaf extract was progressively combined with 50 mL of 0.1 M magnesium nitrate solution. As a result, some white precipitates, primarily composed of  $\text{Mg}(\text{OH})_2$ , were identified. To remove any remaining impurities, the material was centrifuged three times with deionized water at 5000 rpm for 10 min. Finally, the precipitate was dehydrated at 100 °C and calcined at 400 °C to yield MgONPs (Oladipo et al. 2017).

### 16.5.2 Characterization of MgO Nanoparticles

Several methods were used to characterize the MgONPs, including morphological structure and aggregation state analysis. Nanoparticles were irregularly spherical and had a size distribution of 100 nm. Nanoparticles, on the other hand, tended to clump together in stacks, as shown by TEM pictures of the nanoparticle morphology, showing poor dissolvability because of van der Waals (vdW) force (Stabryla et al. 2018). The SAED pattern of MgONPs confirms the material's nanocrystalline structure as well as its ability to be archived into the cubic structure of MgONPs, which is consistent with XRD analysis (Makhluf et al. 2005). In HRTEM image, the interplanar distance between interlayer outskirts is 0.237 nm. The (111), (200), (220), (311), and (222) crystallographic planes of face-centered cubic (FCC)-structured MgO nanoparticles were attributed to only a few strong peaks situated at 36.95, 42.92, 62.30, 74.76, and 78.61, respectively, according to classic XRD spectra (Fig. 16.1a–e).

### 16.5.3 Fungitoxic Mechanism of MgO Nanomaterials

Among all testing conditions, MgONPs reduced both fungi's mycelial development, exhibiting significant concentration-dependent toxic impacts that were consistent with many other metallic nanomaterials (Sun et al. 2018). On the third day, the mean mycelial size of colonies grown on plates containing 125–500 g/mL nanoparticles were 2.1, 1.32, and 0.63 cm, and on the fifth day, it was 5.84, 3.17, and 0.63 cm for *P. nicotianae*; these were much lower groups (Fig. 16.2a). Untreated samples, on the other hand, obtained values of up to 6.21 and 8.3 cm at similar intervals. *T. basicola* mycelia grew slowly in comparison to controls, and flagellated colony expansion was significantly reduced after 10 and 20 days of incubation, with 1.89 and 3.18 cm after 250 g/mL MgONPs, and 2.09 and 2.96 cm after 500 g/mL MgONPs (Fig. 16.2b). Despite the fact that 125 g/mL MgONPs also had no effect on colony size, closer examination revealed a loosening of the mycelial structure as compared to the control group's thick and dense colony. Both fungi's hyphae developed slowly after 5 and 20 days of incubation. In comparison, we used the same approach to investigate the biocidal activity of mMgO (Makhluf et al. 2005).

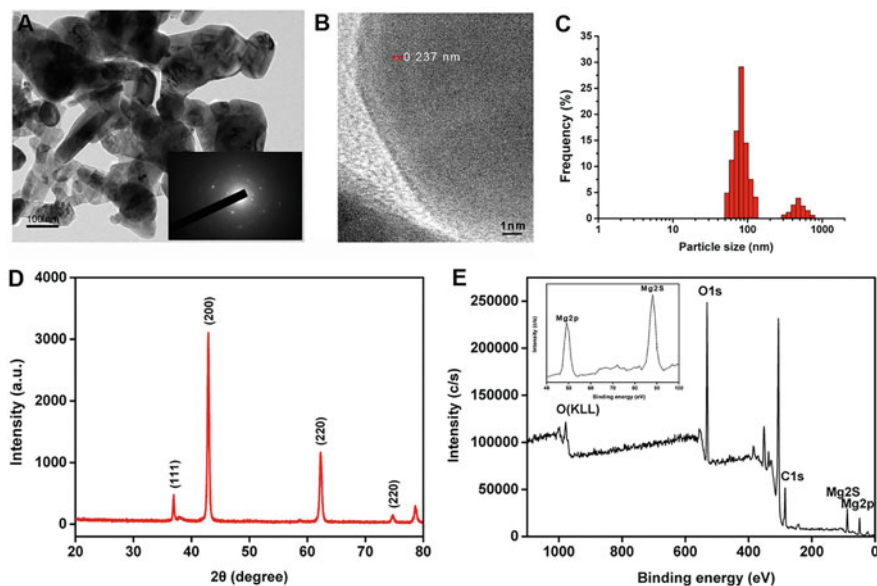


**Fig. 16.1** (a) Inset of representative transmission electron microscopy (TEM) photos of produced MgO nanomaterials with selected area electron diffraction (SAED) patterns (MgONPs). (b) High magnification of MgONPs. (c) Size distributions of nanoparticles (D,E) X-ray diffraction (XRD) and X-ray photoelectron spectroscopy (XPS) survey spectrum of nMgO. The inset plot indicates the strong XPS scan spectrum of nanoparticles in Mg 2p and Mg 2s spectral areas (Chen et al. 2020)

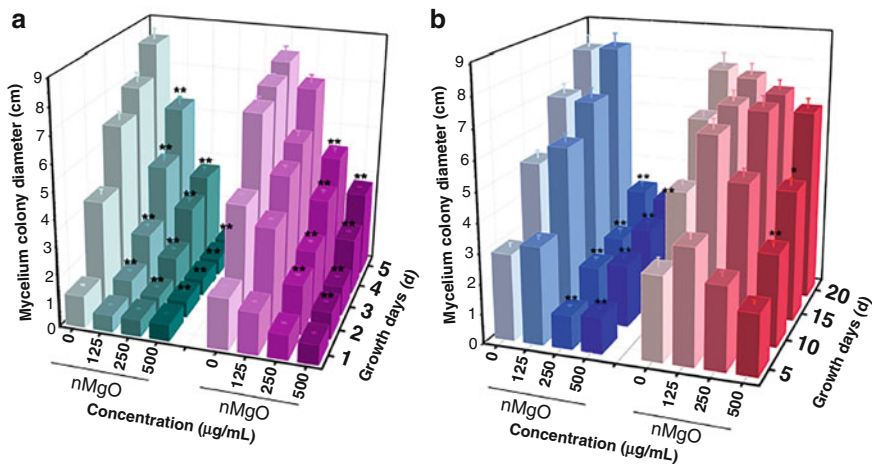


**Fig. 16.2** *P. nicotianae* (a) and *T. basicola* (b) mycelium colony diameter upon 5 and 20 days of application to oatmeal agar (OA) and potato dextrose agar (PDA) media varying concentrations (0, 125, 250, 500 g/mL) of MgO particles or (MgONPs) particles, respectively (Chen et al. 2020)

The results demonstrated that mMgO followed the same concentration-dependent pattern as two types of fungus that were treated with MgONPs. Surprisingly, *P. nicotianae* hyphae growth was substantially hindered, despite *T. basicola* toxicity being quite low. Diameters of two hyphal colonies cultivated for 10 and 20 days in media containing 125 and 250 g/mL mMgO, respectively, compared with those of control were not statistically different, while control exhibited thinner mycelia. Especially for *T. basicola* and *P. nicotianae* growth inhibition rates were 29.63%, 61.8%, 92.4% and 0%, 60.88%, 63.59%, upon MgONPs treatment for 5 and 20 days, whereas mMgO treatment caused 11.46%, 40.0%, 84.80% and 2.91%, 10.00%, 16.10% inhibition rates. In other words, as the incubation time increased, the growth suppressive impact of nanoparticles became stronger. It's possible that when original normal hyphae came into contact with MgONPs, they were severely injured, and the compromised fungal hyphae kept growing, but at a much slower rate. During the incubation period, it appears that the antifungal activity of nanoparticles diminished progressively. Importantly, the antifungal activity of MgONPs was dose-dependent, similar to other metallic oxide nanoparticles and carbon-based nanomaterials (Chen et al. 2016a). It's worth noting that mMgO fungistatic activity was not as high as that caused by MgONPs. Metal oxide nanoparticles have been shown to be more harmful to bacteria, fungus, and plants than their bulked counterparts (Heinlaan et al. 2002). TiO<sub>2</sub>, CuO, and ZnO nanoparticles had also exhibited distinct antifungal action against numerous phytopathogens, including *Gloeophyllum trabeum*, *Lycopersicon esculentum*, *Tinea versicolor*, *Botrytis cinerea*, *Fusarium oxysporum*, and *Pseudoperonospora* (Terzi et al. 2016; Hao et al. 2017). It is the result of increased effective surface area, i.e., compact size that enhances the chances of nanoparticles contacting biological samples, allowing for a broad variety of diverse interactions in nanobiosystems. Further theory holds that when nanoparticles interact with biological cells and membranes, they form a variety of cell-nanoparticle interfaces including protein corona creation, particle encasing, or even intracellular utilization (Nel et al. 2009).

#### 16.5.4 Repression of Conidial Spore Germination and Sporangium Formation

Spores are the smallest propagative components of fungal infections; they significantly contribute to the pathogenic achievement of hosts and have a modest dormant survival potential, such that spore regeneration is required; this is the most important stage in the development of vegetative and reproductive protonema. In the following study, to further test the fungicidal efficiency of nanomaterials, conidial spores of fungal species were assessed for the existence of MgONPs and mMgO (Judelson and Blanco 2005). Microscopy photos of *T. basicola* and *P. nicotianae* spore detentions after incubation with various concentrations demonstrated a significant reduction in spore germination rate, when compared to untreated fungus acting as control samples (approximately complete germination). There was no germination when fungal spores were incubated at their greatest dosage, indicating that they had

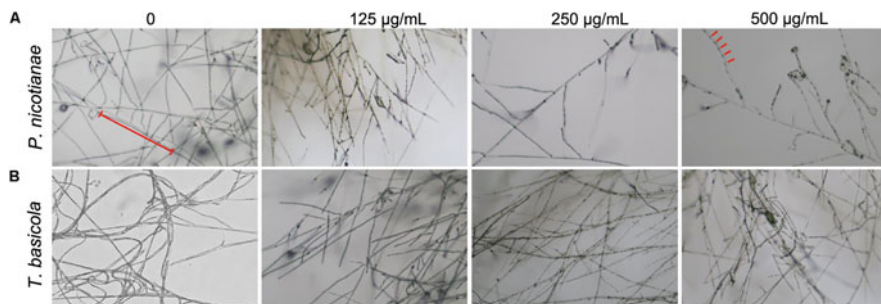


**Fig. 16.3** Microscopic photos of *P. nicotianae* (a, b) and *T. basicola* (c, d) sporangia after co-culture with tested concentrations of MgONPs and micro-Mgo particles, respectively (Chen et al. 2020)

complete sporicidal effects. The MgONPs have shown a stronger sporicidal effect than MgONPs and that the antagonistic impact on spore development is as strong as the effect on mycelial growth. On the other hand, MgONPs had a significant impact on sporangium production. As shown in Fig. 16.3, sporangia of *T. basicola* and *P. nicotianae* developing in the control group contained a lot of conidia. Nevertheless, the number of sporangia and their morphology pattern were significantly reduced in the MgONPs-exposed group at the concentrations tested, which can be attributed to the hypothesis that profoundly directs nanomaterial-hyphae interaction; this disrupts cellular protein and chemical characteristics that are implicated in sporangium forming (Chen et al. 2016a). The *T. basicola* sporangial wall's outer electron-dense layer had disappeared, and the sporangium's structure was loosening (red arrow). However, after 500 g/mL of mMgO treatment, there was a moderately substantial suppression of sporangia production, indicating that mMgO had a mild fungistatic impact (Fig. 16.3). In vivo and in vitro, metals, metal oxide nanomaterials, single-walled carbon nanotubes (SWCNTs), multi-walled carbon nanotubes (MWCNTs), and graphene have all been shown in studies to have sporicidal properties against a variety of phytopathogenic fungi (Liu et al. 2017a, b).

Wani and Shah (2012) observed the nanotoxicity of MgONPs on many agricultural pathogenic fungi and considerable suppression of spore development of *Mucor plumbeus*, *Rhizopus stolonifer*, *F. oxysporum*, and *Alternaria alternata*. MgONPs were recently discovered to inhibit sporulation in seven distinct rot-causing fungi (*Aspergillus alternata*, *Aspergillus niger*, *M. plumbeus*, *Trichothecium roseum*, *Penicillium chrysogenum*, *Rhizoctonia solani*, and *Penicillium expansum*) with no reason. Also, a comparative toxicity experiment was performed on metal nanoparticles' antifungal effectiveness toward seven species of major foliar and soilborne plant diseases, including *B. cinerea*, *A. alternata*, *Verticillium dahlia*, *Monilinia fructicola*, and *Fusarium solani*. Copper nanoparticles (CuNPs) have been found to be most impactful on the majority of fungal spores studied, followed by zinc oxide nanoparticles (ZnONPs), which were also more poisonous than advertising fungicide  $\text{Cu}(\text{OH})_2$  (Malandrakis et al. 2019).

Nevertheless, there was no proof of their antifungal mechanisms. In this respect, we discovered that MgONPs can inhibit sexual reproduction in fungal cells, and future research will look into why MgONPs causes such great sensitivity in fungal cells.

### 16.5.5 Direct Physical Connection of Nanoparticles with Fungal Cells

Several investigations have shown that manufactured nanomaterials come into direct contact with biological tests such as bacteria, fungi, and cells, as well as exterior adhesion and cell absorption patterns (Rodriguez-Gonzalez et al. 2016). Certain metal oxide nanomaterials bond to the surfaces of harmful bacteria, as predicted (Jiang et al. 2009). The authors used SEM/EDS to examine morphological changes in live cells and visually detect the existence of nanoparticles on hyphae to investigate the impact of MgONPs on fungal hyphae.

In this experiment, two types of vegetative mycelia were generated and cultured for 3 h with varied quantities of nanoparticles before being supported on the grid and observed. *T. basicola* and *P. nicotianae* were treated with MgONPs at 500 g/mL, which resulted in clearly undesirable changes after crumbled morphologies under SEM upon exposure. That preserved a filled, uniform, and well-developed tube-like formation. Sunken and bloated, mycelia developed an aberrant structure. In this experiment, two types of vegetative mycelia were generated and cultured for 3 h with varied quantities of nanoparticles before being supported on the grid and examined. *T. basicola* and *P. nicotianae* were exposed to MgONPs at 500 g/mL, which resulted in a clearly undesired alteration, which preserved a complete, consistent, and well-developed tube-like shape under SEM upon treatment. Mycelia sunk and bloated, and they evolved an abnormal structure. EDS was utilized to evaluate if ether MgONPs was present in or on fungi, or to validate the chemical makeup of associated agglomerates because it could trace the atomic number of every atom in a substance (Rodriguez-Gonzalez et al. 2016).

Furthermore, the presence of MgONPs on the hyphal exterior has been established, resulting in cell membrane local disruption. The presence of MgONPs in the cell membrane was investigated as well. These findings back up the theory that metal-based nanoparticles have particle-specific antifungal mechanisms (Stabryla et al. 2018). Furthermore, TEM photos demonstrated that regulated fungal mycelia had normal dense cytoplasm with regular organelle distribution and typical inner and outer cell wall layers.

In summary, the first steps are thought to be harmful to the exterior cell membrane and downregulation of the cellular membrane; as a result, a sequence of essential reactions occur, including successive nanomaterial uptake and communication to biological components such as lipids, DNA, and protein, leading to apoptosis. Aggregation circumstances, geometry, size, and physical qualities all influence the inactivation effects of nanoparticles (Herd et al. 2013). Numerous studies using nanomaterials which physically coated and permeated bacterial membranes demonstrated that they behaved differently than one's microscale aggregates, such as  $\text{Al}_2\text{O}_3$  or  $\text{SiO}_2$  in comparison to their microscale aggregates (Xue et al. 2014). It



appears that understanding the underlying mechanism requires mechanistic interfacial contact among nanoparticles and biological membranes (Sharma et al. 2015). Cell wall structure and composition of fungus could be to blame for these events. Chitin, 1,3 glucans, and 1,6 glucans, as well as a variety of glycoproteins, make up the hyphal cell wall (Brown et al. 2015). Adhesins, or glycoproteins, play a role in adhesion to inorganic or organic surfaces, as well as host–pathogen interactions. Agglutinin-like sequence (ALS) and glycosylphosphatidylinositol (GPI)-modified cell membrane protein families are two main members (Bamford et al. 2015). Nanoparticles, for instance, can behave like promoters, encouraging direct interaction in the same way as carbon nanotubes (CNTs) drive pathogen agglomeration. Sugar-based ligands have been added to CNTs, which are recognized by receptors on *Bacillus* spore surfaces (Luo et al. 2009).

### 16.5.6 Membrane Destabilization in Fungal Cells

In addition, the contribution of glycoproteins to the negative charge of the fungal cell wall cannot be overlooked. Outstanding nanoparticle–cell aggregates that have been found in previous findings of the antibacterial activity of a series of nanoparticles could be mediated by electrostatic contact (Chen et al. 2016a, b). MgONPs and graphene were discovered to be directly bound to phytopathogens, altering cell membrane potential and energy metabolism (Cai et al. 2018). Enhanced adhesion caused by MgONPs adsorption on fungal cells should, in theory, alter membrane potential. Pan et al. (2013) suggest that the Zeta potential of fungal cells has been altered by electrostatic forces among positive-charged MgONPs and fungi, allowing MgONPs to come into close contact with the cell surface and deposit (Pan et al. 2013). Reduced electric repulsive forces resulted in improved antifungal medication adhesion to microorganisms. As a result, as indicated by the SEM and TEM photos discussed above, nanoparticles may be capable of physically harming the cell envelope (Sharma et al. 2015). Leung et al. (2014) discovered that MgONPs effectively conversed with *Escherichia coli*, causing downregulation of membrane proteins like connection porins and ion channel proteins and disruption of proteins associated with membrane lipid metabolism, resulting in cell lysis. Because the internal membrane was directly touched by MgONPs, the nanoparticle–cell interface was extremely diversified. Nanomaterials, afterwards, stimulated vibrant physiochemical conversations that were motivated by adhesion forces that could emerge from specific or non-specific conversations like electrostatic, hydrophobic forces, twisting, vdW, and deforming membranes and rising cytoplasmic membrane permeability to nanomaterials (Wu et al. 2015).

---

## 16.6 Fungal Cells' Oxidative Stress Responding

More research is needed to investigate if nanoparticles generate subcellular or cell membrane oxidative stressors, which has been previously assumed to be the most conceivable method for nanomaterials in living organisms, given the significant

activity of MgONPs versus fungal cells in response to direct interaction. After treatment with modest concentrations of MgONPs, bacterial *Ralstonia solanacearum* cells accumulated ROS (Cai et al. 2018). This is due to the fact that metal nanoparticles' free radicals can damage lipids in bacterial cell membranes (Lopes et al. 2016). However, when fungal pathogens react with nanoparticles, oxidative stress has not been examined. Various species are reported to be the most prominent indicators of oxidative stress erupting in cellular components, including  $O_2^{\cdot-}$ ,  $H_2O_2$ , and ROS (Rispaill et al. 2014). While two kinds of fungal hyphae have been subjected to a variety of MgONPs levels,  $H_2DCFH$ -DA fluorescence was generated inordinately compared to the control. Once the concentration of MgONPs has been improved, the creation of fluorescence improved, demonstrating that MgONPs do indeed induce the generation of ROS.

---

## 16.7 Bimetallic Nanoparticles: Flow Synthesis and Fungicidal Activity

AgNPs (Długosz et al. 2021) are the most widely characterized nanomaterials. They are particularly active against bacteria and can be applied to a wide range of various products (Peszke et al. 2017). Despite nanosilver's numerous advantages, like small doses adequate to restrict bacteria growth, a vast variety of options, and simplified techniques for generating steady suspensions, substances which would operate well for biocide while restricting nanosilver's negative effects are also being sought (Ahmed et al. 2016). CuNPs which have strong antibacterial and antifungal properties are instances of particles with similar properties to AgNPs (Chatterjee et al. 2014). In addition, CuNPs are less costly and easier to find than AgNPs (Asgar et al. 2018). Basic disadvantage of utilizing CuNPs is the challenge of establishing good suspension with sufficient nanoparticle concentration to guarantee adequate bactericidal activity. The technique of generating CuNPs would be time-consuming, and nanomaterials themselves are often bigger than AgNPs, which could reduce CuNPs biocidal potential (Tan and Cheong 2013).

The combination of AgNPs antibacterial capabilities with CuNPs antifungal qualities allows for the creation of material with a broad spectrum of antimicrobial activity (Kalinska et al. 2019). It is feasible to lower quantities of individual metals while keeping similar antibacterial action by synthesizing a product that contains both components. Single-stage or multi-stage techniques can be used to create bimetal molecules or multi-stage core-shell molecules (Liu et al. 2017a, b). The biological activity of the final substance is affected by the ion reducing sequence. Furthermore, the biocidal characteristics of nanoparticles are dependent on the donation of particular metals to item and molecule form. Hikmah et al. (2016) investigated the microstructure or morphology of silver-copper core-shell nanoparticles as a function of Ag to Cu molar proportions. Depending on the metal concentration, nanoparticles varying in size between 25 and 50 nm were created. The magnitude of CuNPs grew significantly as the proportion of copper in



the material increased. This could be due to CuNPs reduced stability, whereas AgNPs remained unaffected by process conditions, and their size stayed unaltered.

Utilization of copper, silver, and bimetallic nanomaterials results in slow mobile ions into a scheme that is important in antibacterial action. Metal ions release ROS that, among other things, impair the action of cell respiratory enzymes. The presence of thiol groups –SH makes it easier for silver ions to interact with each other, enhancing ROS production. On the one hand, AgNPs interact with the bacterial membrane of cells, injuring it, and on the other side, it helps silver ions enter the cell, deactivating it (Sreeju et al. 2016).

Metal nanoparticle suspensions were created in the microwave reactor's flow system. The experimental system's schematic diagram was previously published (Banach and Długosz 2019). In a continuous microwave flow reactor, metal and bimetallic nanoparticles were synthesized (CMFR). Solutions have been hyped through microwave (Samsung, 100–800 W, 2.45 GHz frequency) using an HPLH dosing micropump (model pulse free). The length and diameter of the glass pipe were 550 mm and 70 mm, respectively. To generate nanomaterials, a flow of metal saline solution has been coupled with a flow of tannic acidic media, followed by the flow of hydroxide solution. The overall current of mixture ranged from 171.5 to 343.0  $\text{lm}^3/\text{s}$  depending on residence time. Metal ion solution, tannic acid solution or alkaline solution had reagent volume ratios of 5:2:3. The final volume of nanomaterials has been 500  $\text{mg}/\text{dm}^3$ .

---

## 16.8 Pectinase-Responsive Mesoporous Silica Nanoparticle Carriers (MSNPs)

To protect crops from pests, a great array of chemical pesticides is used in agriculture around the world. However, upwards of 90% of pesticides are misplaced throughout application due to deterioration parameters such as hydrolysis, light, microbes, temperature, and others. Furthermore, non-systemic pesticides are quickly washed into groundwater by rain and are influenced by immediate exposure to external elements like temperature or ultraviolet rays (Zhu et al. 2018). All of these difficulties pose serious risks to the environment and non-target creatures and the increasing expense of agricultural applications. As a result, it's critical to get insecticides to the right target location in plants without decreasing its potency (Kumar et al. 2014). Nanotechnology can currently improve pesticide transfer and distribution in plants, resulting in increased use efficiency (Kumar et al. 2014). Mesoporous silica nanoparticles (MSNPs) offer a lot of potential as nanocarriers for delivering chemicals to plant cells because of their simplicity of fabrication and surface alteration, high surface area, maximum load performance, bioactivity, and general stability (Sun et al. 2014). As a result, MSNPs have been used in a variety of applications, including the packing of molecules like nucleic acids (Kamegawa et al. 2018), proteins, drugs, or pesticides (Shao et al. 2018). On the other hand, MSNPs still need to be improved in terms of control safety and effectiveness. Initial pesticide discharge from MSNPs, for instance, and lower service performance could both lead

to low control systems (Manzano and Vallet-Regí 2020). As a result, developing MSNPs predicated on an encapsulation strategy could indeed help to avoid the untimely secretion of packed cargo in MSNPs.

Smart stimuli-reacting materials are stimulated by light, redox potential (Tryfon et al. 2019; Liang et al. 2020), pH (Xiang et al. 2018), temperature (Gao et al. 2020), or enzymes (Kaziem et al. 2018). They are good for putting pesticides inside nanoparticles so that they stay stable and can be released for a long time. Because of their biodegradability, eco-friendliness, and ease of availability, natural polymers such as chitosan, cellulose, alginate, pectin, and hyaluronan have been widely used in a variety of sectors (Xu et al. 2018; Pang et al. 2019). Because of its abundance of functional groups that could be altered to convey unique physicochemical characteristics, pectin, or polysaccharide, was used as an intermediary for content delivery methods. Moreover, coating a vehicle with pectin, which could be broken down by plant pathogen-secreted enzymes like pectinase, enables pesticide release over a lengthy period of time. Pathogens which induce apoptosis, besides damaging plant cell walls, frequently use the pectin secretion mechanism (Fan et al. 2017).

Rice (*Oryza sativa* L.) is the significant yield that feeds over half of the world's inhabitance. Rice blast disease, induced by *Magnaporthe oryzae*, is among the most damaging diseases to rice, resulting in 80–100% production losses in epidemic areas (Hendy et al. 2019). Rice blast can affect different sections of the rice plant, including leaf collars, pedicels, panicles, seeds, leaves, or necks, causing symptoms and lesions. Rice blast is combated with a variety of pesticides, including nonsystemic insecticides. Efficiency of insecticides against rice blast could be increased by using transport features of nanomaterials in plants. Among other cell wall components, *M. oryzae* produces enzymes that break down cellulose, hemicellulose, cutin, and pectin (Quoc and Bao Chau 2017). Scientists have utilized these enzymes as stimuli throughout investigations on the sustained releasing of pesticides on regular basis (Liang et al. 2020).

Prochloraz (*N*-propyl-*N*-(2-(2,4,6-trichlorophenoxy)ethyl)-imidazole-1-carboxamide) (Pro) is an imidazole fungicide that is proudly utilized to protect plants from a wide range of fungi, including *M. oryzae* (Quoc and Bao Chau 2017). This substance is a 14-demethylation inhibitor that inhibits the CYP51 enzyme encrypted by the CYP51 gene. Pro is a nonsystemic fungicide of low plant uptake, due to ineffective use of field capacity (Zhao et al. 2018a, b). The purpose of this study was to look into the migration and allocation of Pro-loaded MSNPs that had been cross-linked by pectin (Pro@MSN-Pec) throughout rice plants. MSNPs have been produced or fluorescein isothiocyanate (FITC) labeled tracking the carriers' migration through rice plants utilizing optical microscopy. Pro@MSN-Pec and/or commercial formulation antifungal and hybridization characteristics were examined further. Upon revealing rice leaves to Pro@MSN-Pec and commercial formulations, the pro-content in rice plant organs has been determined using high-performance liquid chromatography (HPLC). Utilizing ultrahigh-performance liquid chromatography/mass spectrometry (UPLC/MS), the ultimate residue quantities of Pro in the field have been evaluated.

### 16.8.1 Pro@MSN-Pec Synthesis and Characterization

MSN nanoparticles were produced by condensing silica prelude TEOS in the existence of CTAB, resulting in a configuration that served as a pattern for nanomaterial formation. Because of the reactivity of silica, the exterior of nanomaterials is protected by a large number of available  $-OH$  groups, providing a platform for transplanting multipurpose polymers onto the exterior and inner streams of nanomaterials. In this study, APTES was used to alter the surface of MSN to amino ( $-NH_2$ ) clusters via organic silane clusters (Hussain et al. 2013). In addition, Pro in hexane has been packed into MSNPs. Morphology of MSNPs and Pro@SN-Pec was classified using SEM or TEM. SEM and TEM were used to classify the morphology of MSNPs and Pro@SN-Pec. MSNPs have been found to have stable appearance or spherical shape, with noticeable mesoporous configuration. MSNPs ranged in size from 20 to 50 nm. TEM and SEM assessments revealed changes in particle morphology and size between MSNPs and Pro@MSN-Pec after Pro-loaded MSNPs were transplanted with pectin. Shell structure of Pro@MSN-Pec differed from those of MSNPs, implying that pectin overlay was powerfully encased onto the exterior of MSN to great miscibility and unified form. Particles' sizes ranged from 19 to 110 nm, with an estimate of 70.89 nm. FTIR spectroscopy has been used to explore structural maledictions that occurred following the initial transplantation of particles to different functional clusters. FTIR spectrum of MSNPs revealed intense peak at  $1087\text{ cm}^{-1}$  (asymmetric Si-O-Si stretching),  $975\text{ cm}^{-1}$  (Si-O stretching),  $833\text{ cm}^{-1}$  (symmetric Si-O-Si stretching), or  $462\text{ cm}^{-1}$  (bending vibrations) (Hussain et al. 2013). Absorption band at  $1643\text{ cm}^{-1}$  confirmed that  $Si(OH)_4$  remained the dominant Si species in MSNPs. In the spectrum of MSN- $NH_2$ , a novel absorption peak of the amino ( $-NH_2$ ) cluster has been noted at  $1535\text{ cm}^{-1}$ , along with the absorption band of the methylene ( $-CH_2$ ) group at  $2980\text{ cm}^{-1}$ , demonstrating that  $-NH_2$  cluster was effectively connected on MSN exterior. In MSN-NH-pectin spectrum, sharp peaks for the amide ( $-CONH-$ ) bond, including at  $1458\text{ cm}^{-1}$  (C-N), emerged, confirming the creation of conjugate from the reaction between amino clusters of MSN- $NH_2$  and carboxyl clusters of pectin (Liang et al. 2018). Internal plant pathogen stimuli, like pectinase, might dissolve the pectin protective layer around MSNPs, triggers the production of Pro from Pro@MSN-Pec at a specified location and also triggers the delivery mechanism via pectin-cross-linked MSNPs. Pectinase is relatively stable at room temperature and under neutral conditions. Addition of pectinase resulted in significant accumulated discharge of Pro.

### 16.8.2 Pro@MSN-Pec Fungicidal Activity

After 7 days, fungicidal activity results revealed that Pro@MSN-Pec has been more effective than Pro EC and technical Pro (Table 16.1). After 14 days, Pro@MSN-Pec had greater fungicidal activity than Pro EC or technical Pro at the same concentrations (Abdelrahman et al. 2021), which was most likely due to

**Table 16.1** Fungicidal activity of Pro@MSN-Pec, Prochloraz EC, or Prochloraz technical material toward *Magnaporthe oryzae* (Abdelrahman et al. 2021)

Pesticides	Days following treatment	EC50 ± SE (mg/L)	95% Confidence limits (mg/L)	EC90 ± SE (mg/L)	95% Confidence limits (mg/L)
Pro@MSN-Pec	7	0.113 ± 0.004	0.092 ± 0.134	0.657 ± 0.050	0.401 ± 0.906
Prochloraz EC		0.151 ± 0.013	0.085 ± 0.218	1.197 ± 0.113	0.636 ± 1.759
Prochloraz technical		0.196 ± 0.017	0.112 ± 0.280	1.911 ± 0.164	1.096 ± 2.725
Pro@MSN-Pec	14	0.248 ± 0.012	0.191 ± 0.306	2.301 ± 0.049	2.060 ± 2.542
Prochloraz EC		0.453 ± 0.007	0.419 ± 0.486	3.352 ± 0.014	3.283 ± 3.421
Prochloraz technical		0.725 ± 0.024	0.606 ± 0.844	6.339 ± 0.393	4.385 ± 8.294

Notes: EC50 inhibitory level which inhibits 50% of exposure fungus, EC90 inhibitory level which inhibits 90% of exposure fungus, or SE is standard error (all values are mean of triplicates)

Pro@MSN-Pec's ability to decrease active substance deterioration and thus prolong its efficient period. Furthermore, as a result of response to intensifying stimuli, active ingredient's release may become higher and faster over time, resulting in an increase in Pro's fungicidal activity (Liang et al. 2018). In comparison to Pro EC and technical Pro, stimuli-responsive Pro loaded into pectin covered MSNPs had superior and longer-lasting fungicidal efficacy against *M. oryzae*. The percentage of recovery was calculated using the quantity of Pro injected into blank samples. In blank samples spiked with Pro at three fortified concentrations of 1, 10, and 100 mg/kg, correctness of the analytical technique was explored. Pro recoveries in leaves ranged from 70.1% to 86.5%, in stems from 88.7% to 98.8%, or in roots from 91.6% to 97.9%. Relative standard deviation (RSD %,  $n = 3$ ) was utilized to convey the reproducibility of the current process, with an RSD of 8% in all instances. Agilent software determined detection limit (LOD) as observed signal-to-noise ratio (S/N of 3).

### 16.8.3 MSNPs Translocation in Rice Plants

FITC has been transplanted on the exterior of MSNPs and samples have been investigated under fluorescence microscopy to clearly show MSN diffusion in rice plant organs. MSN-FITC has been used to treat rice plant seedlings in hydroponic systems. To cure rice plants, two application methods were used: the first was to cure leaves to guarantee diffusion of MSNPs via leaves to other sections of the rice plant, and the other would be to cure roots to guarantee the transition of MSNPs by roots to various parts of the rice plant. These findings suggest that MSNPs can be utilized as pesticide commercial vehicles for plants, which is consistent with reports that MSN-FITC can act quickly via plant parts (Zhu et al. 2018). Furthermore, previous research has demonstrated that MSNPs can transport particles inside plants (Sun et al. 2014).

### 16.8.4 Pro Distribution in Rice Plants

Pro@MSN-Pec allocation conduct showed that Pro might be transmitted via rice plant organs like stems, roots, or leaves. The content of Pro throughout leaves handled by Pro@MSN-Pec has been greater than in leaves handled with advertising Pro over a duration of 4 h to 14 days (Abdelrahman et al. 2021). Furthermore, the concentration of Pro in handled leaves peaked on the first day of diagnosis and afterwards gradually declined from 1 to 14 days. From 4 h to 14 days, fungicide was detected through stems or roots. Such findings suggest that Pro might be transmitted through various regions of rice organs. In terms of uptake and accumulation in rice leaves, stems, or roots, Pro@MSN-Pec outperformed traditional Pro EC. Furthermore, Pro quantities in stems or roots peaked on the third day of diagnosis and subsequently declined for 3–14 days. Several studies found that pectin encasing all over Pro-loaded MSNPs might preserve or extend the active ingredient's

**Table 16.2** Last residue amounts of prochloraz in rice plant stems, roots, seeds, leaves, or soil (Abdelrahman et al. 2021)

Compound	Residues (mg/kg)				
	Stems	Roots	Rice seeds	Leaves	Soil
Pro@MSN-Pec (1 g/L)	0.004	0.015	0.004	0.004	0.004
Pro@MSN-Pec (2 g/L)	0.004	0.017	0.004	0.020	0.004
Pro@MSN-Pec (4 g/L)	0.004	0.026	0.011	0.027	0.004
Prochloraz EC (2 mL/L)	0.009	0.015	0.004	0.006	0.004

efficient period, particularly after the third day to 14 days, when contrasted to Pro EC treatment. Particles smaller than 100 nm may also be easily transported into plant tissues (Zhao et al. 2018a, b; Avellan et al. 2019). These particles may contain compounds that plants are unable to absorb, such as pesticides, particularly nonsystemic insecticides, which may enhance their game and extend the active ingredient's lifetime in field treatments against target pests (Zhu et al. 2018).

### 16.8.5 Pro Residues in Various Sections of Rice or Soil Below Field Conditions

Prior to harvest, pro content was evaluated across several areas of the rice plant, including stems, leaves, roots, seeds and soil (Table 16.2). Residue quantities in rice stems, leaves, or roots have been marginally greater than in rice leaves, stems, or roots handled to advertise Pro EC 44%, but residue amounts in seeds or soil are the same. There was a slight difference in the Pro@MSN-Pec levels in rice plants when different Pro@MSN-Pec levels were compared. The highest residue levels found in the 2RD treatment residue limit (MRL) for Pro through rice calculated by the European Union, Japan, China, and Hong Kong were 0.5, 1, and 0.5 mg/kg, respectively. When residue values were contrasted to MRLs, it was found that final Pro concentrations in rice were below maximum allowable concentrations, implying that Pro@MSN-Pec treatment on rice organs presented a minimal risk.

## 16.9 Conclusion

Plant breeding and IPM are currently insufficient agricultural approaches, and innovative alternative solutions that can fulfill our present and future food demands are needed. Investing in cutting-edge agronanotechnology research that is just a couple of decades old is worthwhile. We could save money on plant protection chemicals, reduce yield losses, and increase agricultural productivity by using NPs. The method is sufficient for dealing with issues such as rising chemical input costs,

ineffectual pesticide use, and pesticide contamination of land and groundwater. Because zero-valent iron nanoparticles have a strong attraction to organic molecules or heavy metals, they could be used to remediate pesticide-infested soil. Additionally, FeNPs, like  $\text{CaCO}_3$ , have excellent soil-binding properties. Furthermore, in order to reduce the environmental impact of NM manufacturing, greater emphasis needs to be placed on using agricultural residues as raw resources. Advances in nanobiotechnology, such as the use of green chemistry to synthesize nanoparticles from living tissues and plant extracts, provide guarantees of environmental protection. The diverse potential of nanoparticles includes one's use as vehicles for active targeting of antimicrobial substances and, moreover, one's inherent antimicrobial impacts and properties, both of which prove their own utility when used as nanopesticides or nanofungicides toward plant pathogens.

**Acknowledgments** This work was supported by the Deanship of Scientific Research, Vice Presidency for Graduate Studies and Scientific Research, King Faisal University, Saudi Arabia (GRANT76).

---

## References

- Abdelrahman TM, Qin X, Li D, Senosy IA, Mmby M, Wan H, Li J, He S (2021) Pectinase-responsive carriers based on mesoporous silica nanoparticles for improving the translocation and fungicidal activity of prochloraz in rice plants. *Chem Eng J* 404:126440. <https://doi.org/10.1016/j.cej.2020.126440>
- Ahmad H, Rajagopal K, Shah AH, Bhat AH, Venugopal K (2017) Study of bio-fabrication of iron nanoparticles and their fungicidal property against phytopathogens of apple orchards. *IET Nanobiotechnol* 11(3):230–235. <https://doi.org/10.1049/iet-nbt.2015.0061>
- Ahmad H, Venugopal K, Rajagopal K, De Britto S, Nandini B, Pushpalatha HG, Konappa N, Udayashankar AC, Geetha N, Jogaiah S (2020) Green synthesis and characterization of zinc oxide nanoparticles using eucalyptus globules and their fungicidal ability against pathogenic fungi of apple orchards. *Biomol Ther* 10(3):1–13. <https://doi.org/10.3390/biom10030425>
- Ahmed S, Ahmad M, Swami BL, Ikram S (2016) A review on plants extract mediated synthesis of silver nanoparticles for antimicrobial applications: a green expertise. *J Adv Res* 7:17–28. <https://doi.org/10.1016/j.jare.2015.02.007>
- Albornoz C, Jacobo S (2006) Preparation of a biocompatible magnetic film from an aqueous ferrofluid. *J Magn Magn Mater* 305:12–10
- Ales PC, Milan K, Renata V, Prucek R, Soukupová J, Krystof V, Hamal P, Zboril R, Kvítek L (2009) Antifungal activity of silver nanoparticles against *Candida* spp. *Biomaterials* 30:6333–6340
- Asghar MA, Zahir E, Shahid SM, Khan MN, Asghar MA, Iqbal J, Walker G (2018) Iron, copper and silver nanoparticles: green synthesis using green and black tea leaves extracts and evaluation of antibacterial, antifungal and aflatoxin B1 adsorption activity. *LWT* 90:98–107. <https://doi.org/10.1016/j.lwt.2017.12.009>
- Avellan A, Yun J, Zhang Y, Spielman-Sun E, Unrine JM, Thieme J, Li J, Lombi E, Bland G, Lowry GV (2019) Nanoparticle size and coating chemistry control foliar uptake pathways, translocation, and leaf-to-rhizosphere transport in wheat. *ACS Nano* 13:5291–5305
- Bahadory M (2008) Synthesis of noble metal nanoparticles. PhD thesis, pp 86–153
- Bamford CV, Nobbs AH, Barbour ME, Lamont RJ, Jenkinson HF (2015) Functional regions of *Candida albicans* hyphal cell wall protein Als3 that determine interaction with the oral

- bacterium *Streptococcus gordonii*. Microbiology 161:18–29. <https://doi.org/10.1099/mic0083378-0>
- Banach M, Długosz O (2019) Continuous production of silver nanoparticles and process control. J Clust Sci 30:541–552. <https://doi.org/10.1007/s10876-019-01505-y>
- Bramhanwade K, Shende S, Bonde S, Gade A, Rai M (2016) Fungicidal activity of Cu nanoparticles against *Fusarium* causing crop diseases. Environ Chem Lett 14:229–235. <https://doi.org/10.1007/s10311-015-0543-1>
- Brown L, Wolf JM, Prados-Rosales R, Casadevall A (2015) Through the wall: extracellular vesicles in gram-positive bacteria, mycobacteria and fungi. Nat Rev Microbiol 13:620–630. <https://doi.org/10.1038/nrmicro3480>
- Cai L, Chen JN, Liu ZW, Wang HC, Yang HK, Ding W (2018) Magnesium oxide nanoparticles: effective agricultural antibacterial agent against *Ralstonia solanacearum*. Front Microbiol 9:790. <https://doi.org/10.3389/fmicb.201800790>
- Castro ML, Ojeda C, Cirelli A (2013) Advances in surfactants for agrochemicals. Environ Chem Lett 12:85–95
- Chalkidou A, Simeonidis K, Angelakeris M, Samaras T, Martinez-Boubeta C, Balcells L, Papazisisb K, Dendrinou-Samarac C, Kalogiroua O (2011) *In vitro* application of Fe/MgO nanoparticles as magnetically mediated hyperthermia agents for cancer treatment. J Magn Magn Mater 323:775–780. <https://doi.org/10.1016/j.jmmm.201010043>
- Chang R, Yu J, Ma X, Anderson D (2011) Polysaccharides as stabilizers for the synthesis of magnetic nanoparticles. Carbohydr Polym 83(2):640–644
- Chatterjee AK, Chakraborty R, Basu T (2014) Mechanism of antibacterial activity of copper nanoparticles. Nanotechnology 25:135101. <https://doi.org/10.1088/0957-4484/25/13/135101>
- Chen H, Yada R (2011) Nanotechnologies in agriculture: new tools for sustainable development. Trends Food Sci Technol 22(11):585–594
- Chen JN, Peng H, Wang XP, Shao F, Yuan ZD, Han HY (2014) Graphene oxide exhibits broad-spectrum antimicrobial activity against bacterial phytopathogens and fungal conidia by intertwining and membrane perturbation. Nanoscale 6:1879–1889. <https://doi.org/10.1039/c3nr04941h>
- Chen L, Song Y, Tang B, Song X, Yang H, Li B, Zhao Y, Huang C, Han X, Wang S, Li Z (2015) Aquatic risk assessment of a novel strobilurin fungicide: a microcosm study compared with the species sensitivity distribution approach. Ecotoxicol Environ Saf 120:418–427. <https://doi.org/10.1016/j.ecoenv.2015.06.027>
- Chen JN, Sun L, Cheng Y, Lu ZC, Shao K, Li TT, Han H, Hu C (2016a) Graphene oxide-silver nanocomposite: novel agricultural antifungal agent against *Fusarium graminearum* for crop disease prevention. ACS Appl Mater Interfaces 8:24057–24070. <https://doi.org/10.1021/acsami.6b05730>
- Chen JN, Li SL, Luo JX, Wang RS, Ding W (2016b) Enhancement of the antibacterial activity of silver nanoparticles against phytopathogenic bacterium *Ralstonia solanacearum* by stabilization. J Nanomater 2016:1–15. <https://doi.org/10.1155/2016/7135852>
- Chen J, Wu L, Lu M, Lu S, Li Z, Ding W (2020) Comparative study on the fungicidal activity of metallic MgO nanoparticles and macroscale MgO against soilborne fungal phytopathogens. Front Microbiol 11:1–19. <https://doi.org/10.3389/fmicb.2020.00365>
- Chowdappa P, Gowda S (2013) Nanotechnology in crop protection: status and scope. Pest Manage Hortic Ecosyst 19(2):131–151
- Chowdappa P, Kumar NB, Madhura S, Kumar MS, Myers KL, Fry WE, Cooke DE (2013) Emergence of 13\_A2 blue lineage of *Phytophthora infestans* was responsible for severe outbreaks of late blight on tomato in South-West India. J Phytopathol 161(1):49–58
- Długosz O, Sochocka M, Ochnik M, Banach M (2021) Metal and bimetallic nanoparticles: flow synthesis, bioactivity and toxicity. J Colloid Interface Sci 586:807–818. <https://doi.org/10.1016/j.jcis.2020.11.005>



- Dubchak S, Ogar A, Mietelski JW, Turnau K (2010) Influence of silver and titanium nanoparticles on *Arbuscular mycorrhiza* colonization and accumulation of radiocaesium in *Helianthus annuus*. *Span J Agric Res* 8(1):103–108. <https://doi.org/10.5424/sjar/201008S1-1228>
- Eman ME, Ahmed MA, Okash N, Salwa FM, Samaal ED, Khana MA, Mariam HY (2013) Antifungal activity of zinc oxide nanoparticles against dermatophytic lesions of cattle. *Romanian J Biophys* 23:191–202
- Fan C, Guo M, Liang Y, Dong H, Ding G, Zhang W, Tang G, Yang J, Kong D, Cao Y (2017) Pectin-conjugated silica microcapsules as dual-responsive carriers for increasing the stability and antimicrobial efficacy of kasugamycin. *Carbohydr Polym* 172:322–331
- Gao Y, Xiao Y, Mao K, Qin X, Zhang Y, Li D, Zhang Y, Li J, Wan H, He S (2020) Thermoresponsive polymer-encapsulated hollow mesoporous silica nanoparticles and their application in insecticide delivery. *Chem Eng J* 383:123169
- Ghormade V, Deshpande MV, Paknikar KM (2011) Perspectives for nano-biotechnology enabled protection and nutrition of plants. *Biotechnol Adv* 29(6):792–803
- Gnanasangeetha D, Sarala TD (2013) One pot synthesis of zinc oxide nanoparticles via chemical and green method. *Res J Mater Sci* 1:1–8
- Gopinatha V, Mubarak A, Priyadarshini S, Priyadarshini NM, Thajuddin N, Velusamy P (2012) Biosynthesis of silver nanoparticles from *Tribulus terrestris* and its antimicrobial activity: a novel biological approach. *Colloids Surf B Biointerfaces* 96:69–74
- Gotic M, Jurkin T, Music S (2009) From iron (III) precursor to magnetite and vice versa. *Mater Res Bull* 44:2014–2021
- Gruère GP (2012) Implications of nanotechnology growth in food and agriculture in OECD countries. *Food Policy* 37(2):191–198
- Hao Y, Cao XQ, Ma CX, Zhang ZT, Zhao N, Ali A, Hou T, Xiang Zhiqian ZJ, Wu S, Xing B, Zhang Z, Rui Y (2017) Potential applications and antifungal activities of engineered nanomaterials against gray mold disease agent *Botrytis cinerea* on rose petals. *Front Plant Sci* 8:1332. <https://doi.org/10.3389/fpls.2017.01332>
- Heinlaan M, Ivask A, Blinova I, Dubourguier H-C, Kahru A (2002) Toxicity of nanosized and bulk ZnO, CuO and TiO<sub>2</sub> to bacteria *Vibrio fischeri* and crustaceans *Daphnia magna* and *Thamnocephalus platyurus*. *Chemosphere* 71:1308–1316. <https://doi.org/10.1016/j.chemosphere.2007.11.047>
- Hendy AA, Xing J, Chen X, Chen X-L (2019) The farnesyltransferase  $\beta$ -subunit RAM1 regulates localization of RAS proteins and appressorium-mediated infection in *Magnaporthe oryzae*. *Mol Plant Pathol* 20:1264–1278
- Herd H, Daum N, Jones AT, Huwer H, Ghandehari H, Lehr CM (2013) Nanoparticle geometry and surface orientation influence mode of cellular uptake. *ACS Nano* 7:1961–1973. <https://doi.org/10.1021/nn304439f>
- Hikmah N, Idrus NF, Jai J, Hadi A (2016) Synthesis and characterization of silver-copper core-shell nanoparticles using polyol method for antimicrobial agent. *IOP Conf Ser Earth Environ Sci* 36: 012050–012057. <https://doi.org/10.1088/1755-1315/36/1/012050>
- Hussain HI, Yi Z, Rookes JE, Kong LX, Cahill DM (2013) Mesoporous silica nanoparticles as a biomolecule delivery vehicle in plants. *J Nanopart Res* 15:1676
- Jiang W, Mashayekhi H, Xing B (2009) Bacterial toxicity comparison between nano- and micro-scaled oxide particles. *Environ Pollut* 157:1619–1625. <https://doi.org/10.1016/j.envpol.2008.12.025>
- Johnston CT (2010) Probing the nanoscale architecture of clay minerals. *Clay Miner* 45(3):245–279
- Joshi SM, De Britto S, Jogaiah S, Ito S (2019) Mycogenic selenium nanoparticles as potential new generation broad spectrum antifungal molecules. *Biomolecules* 9:419
- Judelson HS, Blanco FA (2005) The spores of phytophthora: weapons of the plant destroyer. *Nat Rev Microbiol* 3:47–58. <https://doi.org/10.1038/nrmicro1064>
- Kalinska A, Jaworski S, Wierzbicki M, Gołębiewski M (2019) Silver and copper nanoparticles—an alternative in future mastitis treatment and prevention? *Int J Mol Sci* 20:1672. <https://doi.org/10.3390/ijms20071672>

- Kamegawa R, Naito M, Miyata K (2018) Functionalization of silica nanoparticles for nucleic acid delivery. *Nano Res* 11:5219–5239
- Kanhd P, Birla S, Gaikwad S, Gade A, Seabra AB, Rubilarcd O, Duran N, Rai M (2014) *In vitro* antifungal efficacy of copper nanoparticles against selected crop pathogenic fungi. *Mater Lett* 115:13–17
- Kaziem AE, Gao Y, Zhang Y, Qin X, Xiao Y, Zhang Y, You H, Li J, He S (2018)  $\alpha$ -Amylase triggered carriers based on cyclodextrin anchored hollow mesoporous silica for enhancing insecticidal activity of avermectin against *Plutella xylostella*. *J Hazard Mater* 359:213–221
- Khan MR, Rizvi TF (2014) Nanotechnology: scope and application in plant disease management. *Plant Pathol J* 13(3):214–231
- Kumar S, Bhanjana G, Sharma A, Sidhu MC, Dilbaghi N (2014) Synthesis, characterization and on field evaluation of pesticide loaded sodium alginate nanoparticles. *Carbohydr Polym* 101:1061–1067
- Leung YH, Ng AMC, Xu XY, Shen ZY, Gethings LA, Wong MT, Chan CMN, Guo MY, Ng YH, Djurišić AB, Lee PKH, Chan WK, Yu LH, Phillips DL, Ma APY, Leung FCC (2014) Mechanisms of antibacterial activity of MgO: non-ROS mediated toxicity of MgO nanoparticles towards *Escherichia coli*. *Small* 10:1171–1183. <https://doi.org/10.1002/sml.201302434>
- Liang Y, Fan C, Dong H, Zhang W, Tang G, Yang J, Jiang N, Cao Y (2018) Preparation of MSNPs-chitosan@prochloraz nanoparticles for reducing toxicity and improving release properties of prochloraz. *ACS Sustain Chem Eng* 6:10211–10220
- Liang Y, Gao Y, Wang W, Dong H, Tang R, Yang J, Niu J, Zhou Z, Jiang N, Cao Y (2020) Fabrication of smart stimuli-responsive mesoporous organosilica nano-vehicles for targeted pesticide delivery. *J Hazard Mater* 389:122075
- Liu X, Wu Y, Xie G, Wang Z, Li Y, Li Q (2017a) New green soft chemistry route to Ag-Cu bimetallic nanomaterials. *Int J Electrochem Sci* 12:3275–3282. <https://doi.org/10.20964/2017.04.61>
- Liu BK, Xue YF, Zhang JT, Han B, Zhang J, Suo XY, Mu L, Shi H (2017b) Visible-light-driven  $\text{TiO}_2/\text{Ag}_3\text{PO}_4$  teterostructures with enhanced antifungal activity against agricultural pathogenic fungi *Fusarium graminearum* and mechanism insight. *Environ Sci Nano* 4:255–264. <https://doi.org/10.1039/c6en00415f>
- Lopes S, Pinheiro C, Soares AMVM, Loureiro S (2016) Joint toxicity prediction of nanoparticles and ionic counterparts: simulating toxicity under a fate scenario. *J Hazard Mater* 320:1–9. <https://doi.org/10.1016/j.jhazmat.2016.07.068>
- Luo PJG, Wang HF, Gu LR, Lu FS, Lin Y, Christensen KA, Yang S-T, Sun Y-P (2009) Selective interactions of sugar-functionalized single-walled carbon nanotubes with *Bacillus Spores*. *ACS Nano* 3:3909–3916. <https://doi.org/10.1021/nn901106s>
- Mahnaz M, Farideh N, Mansor BA, Mohamad R (2013) Green biosynthesis and characterization of magnetic iron oxide ( $\text{Fe}_3\text{O}_4$ ) nanoparticles using seaweed (*Sargassum muticum*) aqueous extract. *Molecules* 18:5954–5964
- Makhluf S, Dror R, Nitzan Y, Abramovich Y, Jelinek R, Gedanken A (2005) Microwave-assisted synthesis of nanocrystalline MgO and its use as a bactericide. *Adv Funct Mater* 15:1708–1715. <https://doi.org/10.1002/adfm.200500029>
- Malandrakis AA, Kavroulakis N, Chrysikopoulos CV (2019) Use of copper, silver and zinc nanoparticles against foliar and soil-borne plant pathogens. *Sci Total Environ* 670:292–299. <https://doi.org/10.1016/j.scitotenv.2019.03.210>
- Manzano M, Vallet-Regí M (2020) Mesoporous silica nanoparticles for drug delivery. *Adv Funct Mater* 30:1902634
- Mesterhazy A, Bartok T, Kaszonyi G, Varga M, Toth B, Varga J (2005) Common resistance to different *Fusarium* spp causing *Fusarium* head blight in wheat. *Eur J Plant Pathol* 112:267–281
- Mishra S, Singh HB (2015) Biosynthesized silver nanoparticles as a nanoweapon against phytopathogens: exploring their scope and potential in agriculture. *Appl Microbiol Biotechnol* 99(3):1097–1107

- Monalisa P, Nayak PL (2013) Green synthesis and characterization of zero valent iron nanoparticles from the leaf extract of *Azadirachta indica* (neem). *World J Nano Sci Technol* 2(1):06–09
- Muneer MBA, Chai PV, Takriff MS, Benamor A, Mohammad AW (2015) Optimization of nickel oxide nanoparticles synthesis through the sol gel method using box–behken design. *Mater Des* 86:948–956
- Nam KT, Lee YJ, Krauland EM, Kottmann ST, Belcher AM (2008) Peptide-mediated reduction of silver ions on engineered biological scaffolds. *ACS Nano* 2(7):1480–1486
- Nandini B, Puttaswamy H, Prakash HS, Adhikari S, Jogaiah S, Nagaraja G (2020) Elicitation of novel trichogenic-lipid nanoemulsion signaling resistance against pearl millet downy mildew disease. *Biomol Ther* 10:25
- Nel AE, Maedler L, Velegol D, Xia T, Hoek EMV, Somasundaran P, Klaessig F, Castranova V, Thompson M (2009) Understanding biophysicochemical interactions at the nano-biointerface. *Nat Mater* 8:543–557. <https://doi.org/10.1038/nmat2442>
- Oladipo AA, Olatunji JA, Adewale SO, Abimbola OA (2017) Bio-derived MgO nanopowders for BOD and COD reduction from tannery wastewater. *J Water Process Eng* 16:142–148. <https://doi.org/10.1016/j.jwpe.2017.01.003>
- Ozcelik BK, Ergun C (2014) Synthesis of ZnO nanoparticles by an aerosol process. *Ceram Int* 40: 7107–7116
- Pan XH, Wang YH, Chen Z, Pan DM, Cheng YJ, Liu ZJ, Lin Z, Guan X (2013) Investigation of antibacterial activity and related mechanism of a series of nano-Mg(OH)<sub>2</sub>. *ACS Appl Mater Interfaces* 5:1137–1142. <https://doi.org/10.1021/am302910q>
- Pang L, Gao Z, Feng H, Wang S, Wang Q (2019) Cellulose based materials for controlled release formulations of agrochemicals: a review of modifications and applications. *J Control Release* 316:105–115
- Parizi MA, Moradpour Y, Roostaei A, Khani M, Negahdari M, Rahimi G (2014) Evaluation of the antifungal effect of magnesium oxide nanoparticles on *Fusarium oxysporum* F. sp lycopersici, pathogenic agent of tomato. *Eur J Exp Biol* 4:151–156
- Peszke J, Dulski M, Nowak A, Balin K, Zubko M, Sułowicz S, Nowak B, Piotrowska-Seget Z, Talik E, Wojtyniak M, Mrozek-Wilczkiewicz A, Malarz K, Szade J (2017) Unique properties of silver and copper silica-based nanocomposites as antimicrobial agents. *RSC Adv* 7:28092–28104. <https://doi.org/10.1039/C7RA00720E>
- Prasad R (2014) Synthesis of silver nanoparticles in photosynthetic plants. *J Nanopart* 2014: 963961. <https://doi.org/10.1155/2014/963961>
- Prasad R (2016) *Advances and applications through fungal nanobiotechnology*. Springer, Cham
- Prasad R, Jha A, Prasad K (2018) *Exploring the realms of nature for nanosynthesis*. Springer International Publishing, Cham. <https://www.springer.com/978-3-319-99570-0>
- Quoc NB, Bao Chau NN (2017) The role of cell wall degrading enzymes in pathogenesis of *Magnaporthe oryzae*. *Curr Protein Pept Sci* 18:1–16
- Raabe RD, Connors IL, Martinez AP (1981) Checklist of plant diseases in Hawaii: including records of microorganisms, principally fungi, found in the states. Hawaii Institute of Tropical Agriculture and Human Resources (CTAHR), information text series 022
- Rispail N, De Matteis L, Santos R, Miguel AS, Custardoy L, Testillano MC, Pérez-de-Luque A, Maycock C, Fevreiro P, Oliva A, Fernández-Pacheco R, Ibarra MR, de la Fuente JM, Marquina C, Rubiales D, Prats E (2014) Quantum dot and superparamagnetic nanoparticle interaction with pathogenic fungi: internalization and toxicity profile. *ACS Appl Mater Interfaces* 6:9100–9110. <https://doi.org/10.1021/am501029g>
- Rodriguez-Gonzalez V, Dominguez-Espindola RB, Casas-Flores S, Patron-Soberano OA, Camposeco-Solis R, Lee SW (2016) Antifungal nanocomposites inspired by titanate nanotubes for complete inactivation of *Botrytis cinerea* isolated from tomato infection. *ACS Appl Mater Interfaces* 8:31625–31637. <https://doi.org/10.1021/acsami6b10060>
- Sangeetha J, Thangadurai D, Hospet R, Purushotham P, Manowade KR, Jogaiah S (2017) Production of bionanomaterials from agricultural wastes. In: Ram P, Manoj K, Vivek K (eds) *Nanotechnology: an agricultural paradigm*. Springer Nature, Singapore, pp 33–58

- Shah AT, Ahmad S, Kashif M, Khan MF, Shahzad K, Tabassum S, Mujahid A (2014) In situ synthesis of copper nanoparticles on SBA-16 silica spheres. *Arab J Chem* 9:537–541. <https://doi.org/10.1016/j.arabcj.2014.02013>
- Shao D, Li M, Wang Z, Zheng X, Lao Y-H, Chang Z, Zhang F, Lu M, Yue J, Hu H, Yan H, Chen L, Dong W-F, Leong KW (2018) Bioinspired diselenide-bridged mesoporous silica nanoparticles for dual-responsive protein delivery. *Adv Mater* 30:1801198
- Sharathchandra RG, Yatish NS, Jogaiah S (2016) Aquaporin-based nano biotechnological materials for water treatment and novel detection technologies for nanoscale emerging pathogens. In: Sharma SC, Nagabhushana H, Anath Raju KS, Premkumar HB (eds) *Current advances in nano materials*. BMSIT, Dayananda Sagar Institutions, Bangalore, India, pp 103–107
- Sharma S, Ahmad N, Prakash A, Singh VN, Ghosh AK, Mehta BR (2010a) Synthesis of crystalline Ag nanoparticles (AgNPs) from microorganisms. *Mater Sci Appl* 1:1–7
- Sharma D, Rajput J, Kaith BS, Kaur M, Sharma S (2010b) Synthesis of ZnO nanoparticles and study of their antibacterial and antifungal properties. *Thin Solid Films* 519:1224–1229
- Sharma D, Ashaduzzaman M, Golabi M, Shriwastav A, Bisetty K, Tiwari A (2015) Studies on bacterial proteins corona interaction with saponin imprinted ZnO nanohoneycombs and their toxic responses. *ACS Appl Mater Interfaces* 7:23848–23856. <https://doi.org/10.1021/acsami.5b06617>
- Shekhawat MS, Ravindran CP, Manokari MA (2014) Biomimetic approach towards synthesis of zinc oxide nanoparticles using *Hybanthus enneaspermus* (L) F Muell. *Trop Plant Res* 1:55–59
- Shetty HS, Sharada MS, Jogaiah S, Aditya Rao SJ, Hansen M, Jørgensen HJL, Tran LSP (2019) Bioimaging structural signatures of the oomycete pathogen *Sclerospora graminicola* in pearl millet using different microscopic techniques. *Sci Rep* 9:15175
- Sierra-Fernandez A, De la Rosa-Garcia SC, Gomez-Villalba LS, Gomez-Cornelio S, Rabanal ME, Fort R, Quintana P (2017) Synthesis, photocatalytic, and antifungal properties of MgO, ZnO and Zn/Mg oxide nanoparticles for the protection of calcareous stone heritage. *ACS Appl Mater Interfaces* 9:24873–24886. <https://doi.org/10.1021/acsami7b06130>
- Sophie L, Delphine F, Marc P, Roch A, Robic C, Elst LV, Muller RN (2008) Magnetic iron oxide nanoparticles: synthesis, stabilization, vectorization, physicochemical characterizations, and biological applications. *Chem Rev* 108:2064–2110
- Sreeju N, Rufus A, Philip D (2016) Microwave-assisted rapid synthesis of copper nanoparticles with exceptional stability and their multifaceted applications. *J Mol Liq* 221:1008–1021. <https://doi.org/10.1016/j.jmolliq.2016.06.080>
- Stabryla LM, Johnston KA, Millstone JE, Gilbertson LM (2018) Emerging investigator series: it's not all about the ion: support for particle specific contributions to silver nanoparticle antimicrobial activity. *Environ Sci Nano* 5:2047–2068. <https://doi.org/10.1039/c8en00429c>
- Sun D, Hussain HI, Yi Z, Siegele R, Cresswell T, Kong L, Cahill DM (2014) Uptake and cellular distribution, in four plant species, of fluorescently labeled mesoporous silica nanoparticles. *Plant Cell Rep* 33:1389–1402
- Sun Q, Li JM, Le T (2018) Zinc oxide nanoparticle as a novel class of antifungal agents: current advances and future perspectives. *J Agric Food Chem* 6:11209–11220. <https://doi.org/10.1021/acs.jafc.8b03210>
- Tan KS, Cheong KY (2013) Advances of Ag, Cu, and Ag–Cu alloy nanoparticles synthesized via chemical reduction route. *J Nanopart Res* 15:1537. <https://doi.org/10.1007/s11051-013-1537-1>
- Terzi E, Kartal SN, Yilgor N, Rautkari L, Yoshimura T (2016) Role of various nano-particles in prevention of fungal decay, mold growth and termite attack in wood, and their effect on weathering properties and water repellency. *Int Biodeterior Biodegradation* 107:77–87. <https://doi.org/10.1016/j.ibiod.2015.11.010>
- Thilagavathi T, Geetha D (2014) Nano ZnO structures synthesized in presence of anionic and cationic surfactant under hydrothermal process. *Appl Nanosci* 4:127–134
- Tournas VH (2005) Spoilage of vegetable crops by bacteria and fungi and related health hazards. *Crit Rev Microbiol* 31(1):33–44

- Tryfon P, Antonoglou O, Vourlias G, Mourdikoudis S, Menkissoglu-Spiroudi U, Dendrinou-Samara C (2019) Tailoring Ca-based nanoparticles by polyol process for use as nematicidal and pH adjusters in agriculture. *ACS Appl Nano Mater* 2:3870–3881
- Ul Haq I, Ijaz S (2019) Use of metallic nanoparticles and nanofertilizers as nanofungicides for sustainable disease management in plants. In: Prasad R, Kumar V, Kumar M, Choudhary D (eds) *Nanobiotechnology in bioformulations, Nanotechnology in the life sciences*. Springer, Cham, pp 289–316. [https://doi.org/10.1007/978-3-030-17061-5\\_12](https://doi.org/10.1007/978-3-030-17061-5_12)
- Valentin VM, Svetlana SM, Andrew JL, Sinitsyn OV, Dudnik AO, Yaminsky IV, Taliatsky ME, Kalinina NO (2014) Biosynthesis of stable iron oxide nanoparticles in aqueous extracts of *Hordeum vulgare* and *Rumex acetosa* plants. *Langmuir* 30(20):5982–5988
- Venkateswarlu S, Rao Y, Balaji T, Prathimaa B, Jyothi NVV (2013) Biogenic synthesis of Fe<sub>3</sub>O<sub>4</sub> magnetic nanoparticles using plantain peel extract. *Mater Lett* 100:241–244
- Villamizar-Gallardo R, Cruz JFO, Ortíz-Rodríguez OO (2016) Fungicidal effect of silver nanoparticles on toxigenic fungi in cocoa. *Pesq Agropec Bras* 51:1929–1936
- Vu HT, Keough MJ, Long SM, Pettigrove VJ (2015) Effects of the boscalid fungicide Filan on the marine amphipod *Allorchestes compressa* at environmentally relevant concentrations. *Environ Toxicol Chem* 35:1130–1137. <https://doi.org/10.1002/etc3247>
- Wang MH, Ma X, Jiang W, Zhou F (2014) Synthesis of doped ZnO nanopowders in alcohol–water solvent for varistors applications. *Mater Lett* 121:149–151
- Wani A, Shah M (2012) A unique and profound effect of MgO and ZnO nanoparticles on some plant pathogenic fungi. *J Appl Pharm Sci* 2:40–44
- Wu W, Lei M, Yang S, Zhou L, Liu L, Xiao X, Jiang C, Roy VAL (2015) One-pot route to alloyed Cu/Ag bimetallic nanoparticles with different mass ratio for catalytic reduction of 4-Nitrophenol. *J Mater Chem A* 3:3450–3455. <https://doi.org/10.1039/C6TA09921A>
- Xiang Y, Zhang G, Chen C, Liu B, Cai D, Wu Z (2018) Fabrication of a pH-responsively controlled-release pesticide using an attapulgite-based hydrogel. *ACS Sustain Chem Eng* 6:1192–1201
- Xiulan W, Lanlan H, Zuliang C, Megharaj M, Naidu R (2013) Synthesis of iron-based nanoparticles by green tea extract and their degradation of malachite. *Ind Crop Prod* 51:342–347
- Xu C, Cao L, Zhao P, Zhou Z, Cao C, Li F, Huang Q (2018) Emulsion-based synchronous pesticide encapsulation and surface modification of mesoporous silica nano-particles with carboxymethyl chitosan for controlled azoxystrobin release. *Chem Eng J* 348:244–254
- Xue JZ, Luo ZH, Li P, Ding YP, Cui Y, Wu QS (2014) A residue-free green synergistic antifungal nanotechnology for pesticide thiram by ZnO nanoparticles. *Sci Rep* 4:5408. <https://doi.org/10.1038/srep05408>
- Zhang X, Cui Z (2009) Synthesis of Cu nanowires via solvothermal reduction in reverse microemulsion system. *J Phys Conf Ser* 152:012022. <https://doi.org/10.1088/1742-6596/152/1/012022>
- Zhao P, Cao L, Ma D, Zhou Z, Huang Q, Pan C (2018a) Translocation, distribution and degradation of prochloraz-loaded mesoporous silica nanoparticles in cucumber plants. *Nanoscale* 10:1798–1806
- Zhao RT, Kong W, Sun MX, Yang Y, Liu WY, Lv M, Song S, Wang L, Song H, Hao R (2018b) Highly stable graphene-based nanocomposite (GO-PEI-Ag) with broad-spectrum, long-term antimicrobial activity and antibiofilm effects *ACS. Appl Mater Interfaces* 10:17617–17629. <https://doi.org/10.1021/acsami8b03185>
- Zhu F, Liu X, Cao L, Cao C, Li F, Chen C, Xu C, Huang Q, Du F (2018) Uptake and distribution of fenoxanil-loaded mesoporous silica nanoparticles in rice plants. *Int J Mol Sci* 19:2854